

Thermal Conductivity Tests

Nicholas Kellaris

May 2, 2013

1 Motivation to Conduct Tests

The next generation of the CDMS Experiment – SNOLab – will require a significant improvement in cold hardware thermal performance (around a factor of ten) to fall within the cooling power of the dilution fridge which will be used. We are at the edge of this threshold now with our current designs, and are therefore very sensitive to the thermal properties of our candidate materials. It is for this reason that we wish to characterize precisely the thermal conductivity of all our candidate materials. Below, I describe the tests which have been conducted, the tests which will be conducted, and the reasoning for our interest in the materials.

1.1 Vespel SCP-5000 and SCP-5050

The DuPont Vespel SCP series materials can be seen as the "updated" SP series from the same manufacturer. SCP-5000 and SCP-5050 are similar to SP-1 and SP-22, respectively, except with higher strength and thermal stability (i.e. lower coefficient of thermal expansion). This naturally makes them very attractive as tower stand-off materials.

1.2 Graphlite Carbon Fiber

Graphlite is a trade name for carbon fiber, which is known for its strength. This material has shown to have an impressively high compressive/tensile strength which would be exploited in a truss structure. A very similar material has been characterized by Marc Runyan at larger diameters.

1.3 Ti 15-3-3-3

Ti 15-3-3-3 is an alloy of titanium created by TIMETAL with composition 15V-3Sn-3Al-3Cr and Ti as a balance. This material has been measured previously in plate form and has shown to have very interesting (and very low) thermal conductivity at low temperatures. In addition, it is a very strong alloy with a low thermal expansion coefficient and superconducting properties. We have interest in Ti 15-3-3-3 in plate, tube, and foil form. We have looked into multiple sources for these forms, each of which must be characterized, due to the different manufacturing processes present in the production of each.

1.4 Mersen Graphite Grade 2020

Mersen's grade 2020 graphite is interesting to us for multiple reasons. First, Mersen manufactures the Graphite we currently use, grade UF-4S, which has low thermal conductivity and high purity. Second, it is a nuclear grade graphite, so should have very low radioactivity – a necessity in our experiment. Third, this grade was specifically recommended to us by the R&D and Technical Manager at Mersen, as well as their resident graphite expert to satisfy low radioactivity and low thermal conductivity requirements.

1.5 POCO Graphites

POCO manufactures many grades of graphites. One of their industrial grades, AXM-5Q has demonstrated very low thermal conductivity. We wish to characterize some of their other industrial grades, ACF-10Q and ZXF-5Q, which may offer similar thermal qualities. Though these graphites are industrial grade, we have demonstrated that they may be purified to acceptable levels of radioactivity.

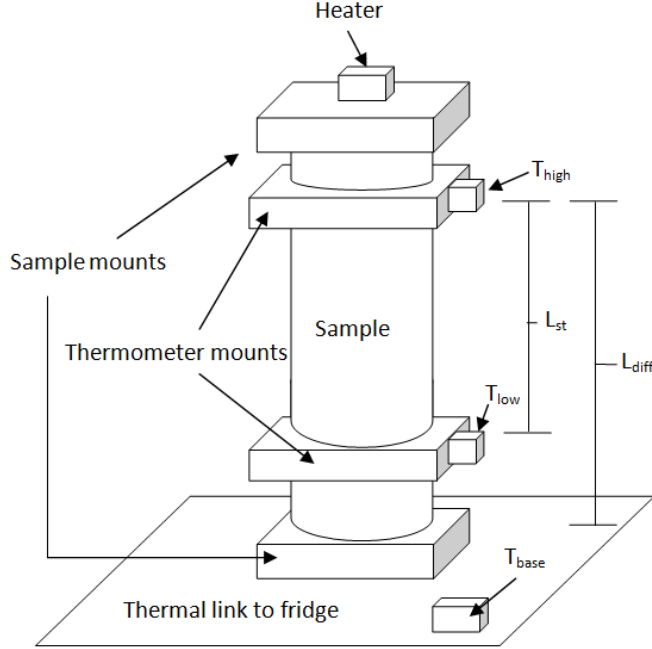


Figure 1: Representative test set-up for thermal conductivity tests performed in the $75\mu\text{W}$ dilution fridge. The sample mounts were gold-plated copper for all samples except the Ti 15-3-3-3, which was unplated copper. All thermometer mounts were copper. Primarily two thermometers (T_{high} and T_{low}) were used for measurements, but a third (T_{base}) was mounted on the thermometry package attached to the tower to verify fridge base temperatures throughout some measurements.

2 Experimental Test Set-up

The thermal conductivity tests were conducted in a $75\text{-}\mu\text{W}$ helium dilution refrigerator. A representative experimental set-up is shown in Figure 1. The samples were connected on one end (through multiple copper-copper interfaces) to the mixing chamber of the fridge, while the other end was thermally isolated.

2.1 Heater

The heater was a metal film resistor, which offers high stability over large temperature ranges. Power was applied to the heater through a Keithley Quad Voltage Source. The resistance was initially $2k\Omega$, but was later switched to $20k\Omega$ to allow greater resolution in the voltage applied to the heater, due to the internal 0.25mV step size from the Keithley. Only the first Graphlite measurement, Vespel SCP-5050, and Vespel SP-22 used the $2k\Omega$ heater.

2.2 Thermometry

Temperature was read out by either two or three thermistors, depending on the test. T_{high} and T_{low} were used in every test; T_{high} was Ge and T_{low} was RuOx. T_{base} was used in some tests to verify the base temperature of the fridge and was a Ge thermistor.

2.3 Wiring

All electrical connections were initially $.003''$ diameter manganin wires. The initial Graphlite measurement, as well as the Vespel SCP-5050 and SP-22 measurements were performed with this wiring. Subsequent tests switched to $.0012''$ manganin wires with a Formvar coating for the Heater and T_{high} connections in order to minimize parasitic heat loads. T_{high} and T_{low} were both four-wire connections for accurate resistance readout.

2.4 Mounting

The samples were epoxy-ed with Stycast-1266 into gold-plated-copper mounts for improved heat transfer from the heater, through the sample, to the fridge. The specific mount design for each sample is shown in Figure 2.

Separate thermometer mounts were fabricated and placed along the sample to avoid any Kapitza resistance effects caused by placing thermometers on the same block as the heater. The thermometer mounts were placed far enough along the sample to be confident that planar heat flow had been established by the time temperature was read out.

3 Methods for Measuring Thermal Conductivity

The thermal conductivity of our samples was measured using three methods which I have termed the "differential" method, the "standard" method, and the "parameter-fit" method. The standard method and the parameter-fit method utilize the same measurements, but different analysis methods, while the differential method is different altogether. All three are outlined below.

3.1 Differential Method

This method for measuring thermal conductivity involves two successive measurements to provide one thermal conductivity data point. First, power P_1 is applied to the sample to establish a gradient, with the "hot" thermometer at some T_{high_1} . Then, more power, P_2 , is applied to the sample which raises the "hot" thermometer to T_{high_2} . Throughout these two measurements, we assume a good enough thermal link to the fridge such that the base of the sample remains roughly constant (whether or not it is at T_{base}). The gradient of interest in both cases is T_{high} to whatever temperature the base of the sample is at (for simplicity we will call it T_{base}). Then in steady state, the power through the sample is,

$$P = \int_{T_{base}}^{T_{high}} \frac{A}{L_{diff}} K(T) dT \quad (1)$$

where T_{base} is the temperature of the cold end of the sample, T_{high} is the temperature of the top thermometer, A is the cross-section of the sample, L_{diff} is the length from the hot thermometer to the base of the sample as shown in Figure 1, and $K(T)$ is the thermal conductivity of the sample. From here, we subtract P_1 from P_2 to obtain an effective integral,

$$\begin{aligned} P_2 - P_1 &= \left(\int_{T_{base}}^{T_{high_2}} \frac{A}{L_{diff}} K(T) dT - P_{parasitic} \right) - \left(\int_{T_{base}}^{T_{high_1}} \frac{A}{L_{diff}} K(T) dT - P_{parasitic} \right) \\ &= \int_{T_{high_1}}^{T_{high_2}} \frac{A}{L_{diff}} K(T) dT . \end{aligned} \quad (2)$$

Here we assume that the thermal conductivity is some integrable function with the same form in both integrals, and $P_{parasitic}$ is some constant parasitic contribution to the heat load (from noise, etc.). Then, upon integration, the value of the integral at the lower limit, T_{base} , cancels out in both integrals, leaving the effective integral at the right of the last equal sign. So, given $P_2 - P_1 = \Delta P$, the differential power, we calculate the thermal conductivity at,

$$T_{avg} = \frac{T_{high_1} + T_{high_2}}{2} \quad (3)$$

by assuming $K(T)$ is nearly constant over the range $T_{high_1} \rightarrow T_{high_2}$ so that it can be brought outside of the integral,

$$\Delta P = K_{T_{avg}} \frac{A}{L_{diff}} \int_{T_{high_1}}^{T_{high_2}} dT . \quad (4)$$

Integrating and rearranging, we have,

$$K(T_{avg}) = \Delta P \frac{L_{diff}}{A(T_{high_2} - T_{high_1})} . \quad (5)$$

This method has several advantages and disadvantages:

Advantages

- As can be seen from eqn 2, any constant parasitic heat load can be neglected with this method, making low temperature measurements (with low applied powers) much easier.
- Since this method only uses one thermometer to do temperature measurements (T_{high}), it eliminates any relative calibration error between thermometers, such as may be present between T_{high} and T_{low} .
- It allows the measurement to be conducted over very small effective gradients ($T_{high_1} \rightarrow T_{high_2}$) so the constant thermal conductivity approximation used in eqn 4 is more accurate, even for strongly temperature-dependent thermal conductivities.

Disadvantages

- The differential method requires a very good thermal link to the cooling bath/a fridge with a high cooling power. This is to ensure that T_{base} is roughly constant between two consecutive measurements. The error from a varying T_{base} is amplified in shorter samples.

3.2 Standard Method

Though there is obviously no "standard" method for measuring thermal conductivity, I refer to this as the standard method as it is the most straight-forward of the steady heat-flow measurement methods. This involves applying a power, P_{heater} , to the top of the sample and letting the sample reach equilibrium (which took anywhere from 30 minutes at higher temperatures to 90 minutes at the lowest temperatures) according to the steady-state heat flow equation,

$$\begin{aligned} P &= P_{heater} + P_{parasitic} \\ &= \int \frac{A}{L_{st}} K(T) dT \end{aligned} \quad (6)$$

where A is the cross-section of the sample, L_{st} is the length between the two thermometers, given in Figure 1, $K(T)$ is the temperature-dependent thermal conductivity of the sample, and $P_{parasitic}$ is any other parasitic heat load through the sample. Reading out the temperatures T_{high} and T_{low} , and assuming that $K(T)$ is nearly constant over this temperature range, we bring $K(T)$ out of the integral as in eqn 4 and integrate. After rearranging we have,

$$K_{T_{avg}} = P \frac{L_{st}}{A(T_{high} - T_{low})} , \quad (7)$$

where $K_{T_{avg}}$ is assumed to be the thermal conductivity at some T_{avg} (defined in eqn 3).

The standard method has its own set of advantages and disadvantages, which are outlined below.

Advantages

- This method is simple, with no assumptions about good thermal links to cooling baths, etc.

Disadvantages

- There is a high sensitivity to relative calibration errors between T_{high} and T_{low} for small temperature gradients, which makes measurements at lower temperatures difficult.
- Constant parasitic heat loads – if not adjusted for in calculations – can be larger than applied heat loads for low temperature ranges, giving hugely inaccurate results for K . The effects of these heat loads can be minimized by either increasing the geometric factor A/L to increase applied heat loads through the sample (decreasing the percentage of power coming from parasitic sources), or by measuring and accounting for $P_{parasitic}$ in calculations.
- Errors from the constant thermal conductivity approximation can grow quickly at large gradients, especially for strongly temperature-dependent thermal conductivities. However, for most thermal conductivities, gradients of over 100% of T_{high} can be used with minimal errors¹.

¹See [?] for a discussion of these errors.

3.3 Parameter-fit Method

The parameter-fit method is similar to the standard method in that a power is applied to that sample, and T_{high} and T_{low} are read out once equilibrium is reached. We start, from eqn 6, but instead of assuming a constant K , we assume some integrable form for $K(T)$ – often a power law of the form $A \cdot T^B$ at sub-kelvin temperatures. We can then vary a set of parameters (e.g. A and B in the power law form) to find those which minimize the quantity,

$$\Delta = \sum_{i=1}^n \frac{P_{total_i} - P_{expected_i}}{P_{total_i}} \quad (8)$$

for n measurements. $P_{total_i} = P_{heater_i} + P_{parasitic_i}$ is a combination of the power applied to the heater and any parasitic heat loads, and $P_{expected_i}$ is given by,

$$P_{expected_i} = \int_{T_{low_i}}^{T_{high_i}} \frac{A}{L_{st}} K(T) dT \quad (9)$$

with T_{high_i} and T_{low_i} being the high and low thermometer temperatures for a given measurement and $K(T)$ is the assumed form for thermal conductivity with certain parameter values. Δ will vary as you vary parameter value combinations. Whichever values minimize this quantity are the best fit to the data.

The standard method approaches the parameter-fit method in the limit of very small gradients, therefore they share similar advantages and disadvantages.

Advantages

- Since this method makes no assumptions about a constant thermal conductivity (unlike the standard method), it isn't susceptible to error for large gradients.
- It makes no assumptions about a perfect thermal link to a reservoir.

Disadvantages

- Since both the high and low thermometers are used, low gradient measurements are sensitive to relative calibration errors between thermometers.
- The data is sensitive to constant parasitic heat loads which can introduce large errors when $P_{parasitic}$ is comparable to P_{heater} .
- This method forces the data to be fit to an assumed form, so the data is inherently more "processed" by the time it is viewed. This could gloss over any anomalous behavior in the material's conductivity curve. Most materials' thermal conductivity, however, can be fit to a power law at low temperatures, so this isn't always a problem.

4 Measured Thermal Conductivities

The thermal conductivities of five samples has been measured as of May 2, 2013. These are: Graphlite carbon fiber, Vespel SCP-5050 & SCP-5000, Vespel SP-22, and Ti 15-3-3-3. The results of each measurement are presented below with a brief discussion following. Note that error bars on the plots have only been included for the standard method. I hope to add errors for the other methods soon.

4.1 Graphlite

The thermal conductivity of a 0.156" diameter Graphlite rod was measured from 0.05K to 0.5K using the three methods described above. The plot is shown in Figure 2. The agreement between all three methods is very good for the case of the Graphlite, as the thermal contact between the fridge and the sample was very good. The parameter-fit method in this case was fit to an altered power law of the form,

$$K(T) = A \cdot T^{(B-C \cdot T^D)} \quad (10)$$



Figure 2: The SP-22 sample-mount interface broke during removal from the fridge. This occurred with hardly any applied force on the sample. The was the interface which affected the thermal link to the fridge as was likely the cause of the discrepancy between the differential method and other methods shown in Figure 4.

which is the same form fitted to in a previous measurement by M. Runyan in [3]. The parameter-fit method, shown in Figure 2, gave a thermal conductivity of,

$$K(T) = 101.2 \cdot T^{(1.93-1.15 \cdot T^{0.28})} \frac{\mu W}{cm - K} \quad (11)$$

for the data range. This is noticeably higher than was measured in [3]. This could be due to the fact that the larger diameter sample measured by M. Runyan was not the "official" Graphlite, as Graphlite is only manufactured up to the 0.156" diameter measured here.

4.2 Vespel SCP-5050

The thermal conductivity of Vespel SCP-5050 was measured from 0.09K to 0.5K. The results are shown in Figure 3 below. Once again, all three methods are in very good agreement, with the parameter-fit method giving a power law fit of

$$K(T) = 10.78 \cdot T^{1.90} \frac{\mu W}{cm - K} . \quad (12)$$

4.3 Vespel SP-22

The thermal conductivity of Vespel SP-22 was measured from 0.1 to 0.3K. The results are plotted and compared to previous measurements of this material in Figure 4. With this sample we can clearly see that the differential measurement is not in agreement with the other two methods. We hypothesize that this was due to a poor thermal link to the fridge caused by improper gluing. We discovered this as the sample broke free of its base mount on the fridge connection side during disassembly with almost no applied force. The break is shown in Figure 5.

The parameter-fit method used a power law fit and gave a thermal conductivity of,

$$K(T) = 13.3 \cdot T^{1.73} \frac{\mu W}{cm - K} \quad (13)$$

which is shown to be in very good agreement with previous measurements of SP-22.

This test was primarily a confirmation of our Vespel SCP-5050 results as it confirmed the accuracy of our test set-up. The equipment used in both tests was identical (same heater, wiring, sample dimensions, etc.) so is a strong confirmation of the SCP-5050 results.

4.4 Vespel SCP-5000

The thermal conductivity of Vespel SCP-5000 was measured from 0.09K to 0.55K using the three methods described in the previous section. Here, the tests were conducted slightly differently, with two differential measurements being performed instead of one. This involved the differential measurement using the T_{high} thermometer only, but also a

separate measurement which utilized the T_{low} thermometer only. This resulted in two differential measurements on different effective sample lengths (one from T_{high} to base and one from T_{low} to base). The results are shown in Figure 6.

In the figure, we see a huge discrepancy between the two differential measurements, as well as between the differential measurements and the other methods. This was likely due to very poor thermal contact with the fridge (possibly caused by untightened mounting screws, or poor gluing). This is evidenced by the fact that the short-sample differential method (using T_{low} suffered a greater error than the long-sample measurement. This test will be re-run at a later date to attempt to rectify this discrepancy.

The parameter-fit method and standard method are once again in good agreement, with the parameter-fit giving a thermal conductivity of,

$$K(T) = 15.2 \cdot T^{1.12} \frac{\mu W}{cm - K} . \quad (14)$$

4.5 Ti 15-3-3-3

The thermal conductivity of Ti 15-3-3-3 is of interest for reasons described in section 1. Since billets of Ti 15-3-3-3 are not available in the United States, we purchased a round billet of Ti 15-3-3-3 from ReTi in China. It the the thermal conductivity of this material which is presented here from 0.07K to 0.3K.

The results of this measurement are shown in Figure 7, alongside measurements of similar samples. We see from the figure that the agreement between the three methods is fair in this case, but there is still a visible discrepancy between the differential method and the other two methods. The reasons for this discrepancy are unknown, but are likely due to a less-than-ideal thermal link to the fridge.

The parameter-fit method gave a thermal conductivity of,

$$K(T) = 187.4 \cdot T^{1.82} \frac{\mu W}{cm - K} \quad (15)$$

which is in good agreement with the measurements performed by M. Runyan on a similar bulk sample of Chinese-sourced Ti 15-3-3-3. The interesting thermal behavior exhibited by TIMET's Ti 15-3-3-3 is not present in this sample, making it much less desirable as a stand-off material.

4.6 Thermal Conductivities of All Materials

The parameter-fit thermal conductivities of all tested materials is presented in Figure 8 below.

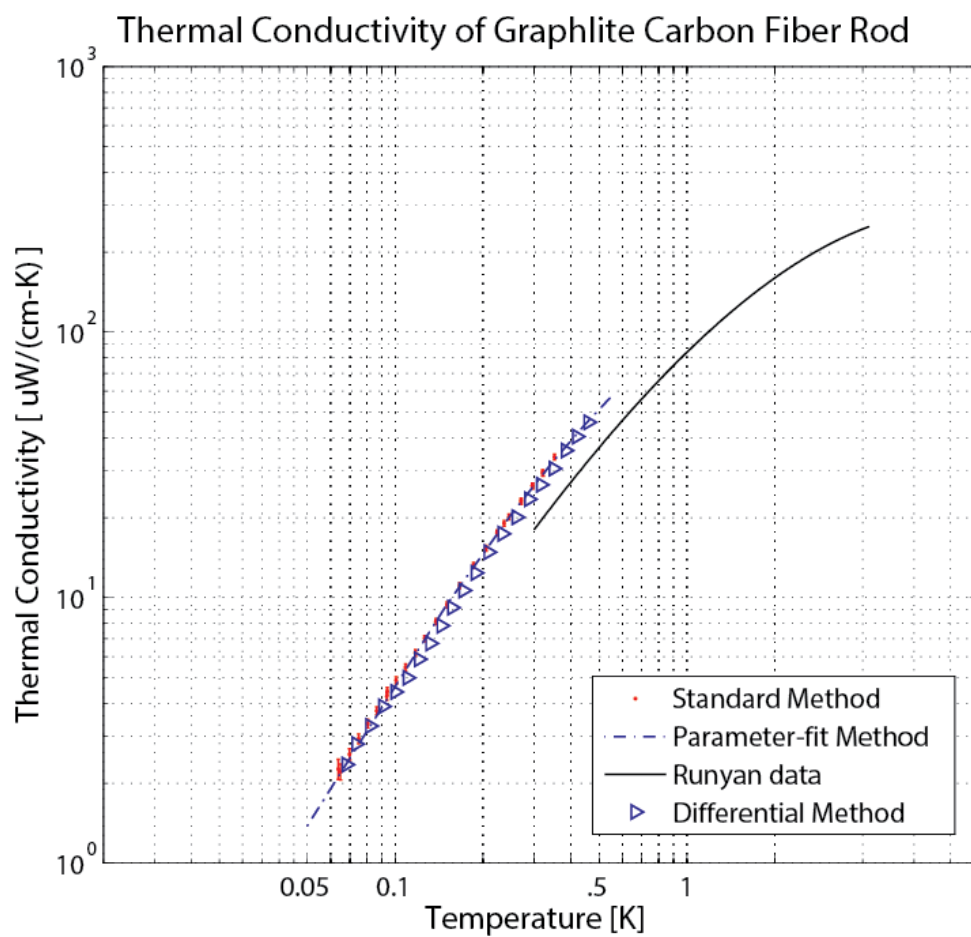


Figure 3: Thermal conductivity of Graphlite from 0.05K to .5K as measured at UC Berkeley. The results are show reasonable agreement with a previous measurement of Graphlite by M. Runyan, plotted as the solid (—) black line [3]. The disagreement could be due to the fact that the sample measured by M. Runyan was not "official" Graphlite, though it was provided by the same company.

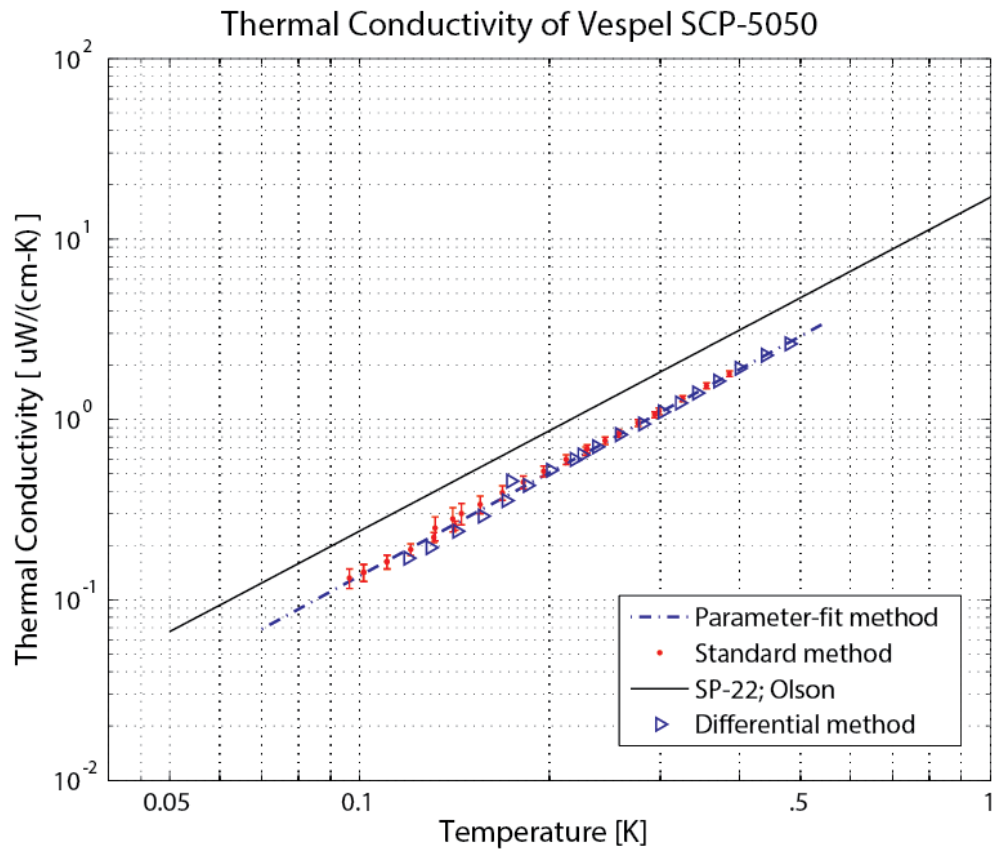


Figure 4: Thermal conductivity of Vespel SCP-5050 as measured from 0.09K to 0.5K. This data is compared to previous measurements of Vespel SP-22 (a very similar material, which we hope SCP-5050 can improve upon) by J.R. Olson [1]. SCP-5050 is noticeably lower ($\sim 30\%$) in thermal conductivity.

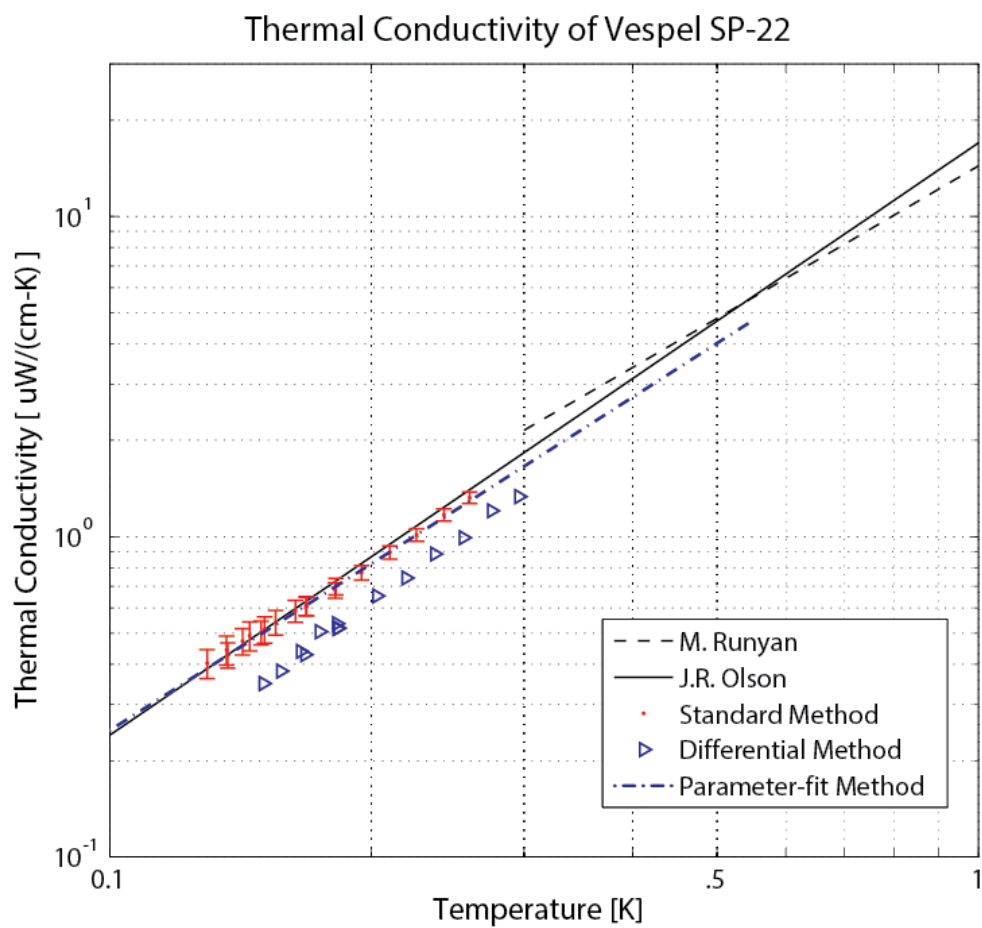


Figure 5: Thermal conductivity measurements of Vespel SP-22 as compared to previous measurements by J.R. Olson. The uncertainty presented for the standard method are very conservative, and are likely lower.

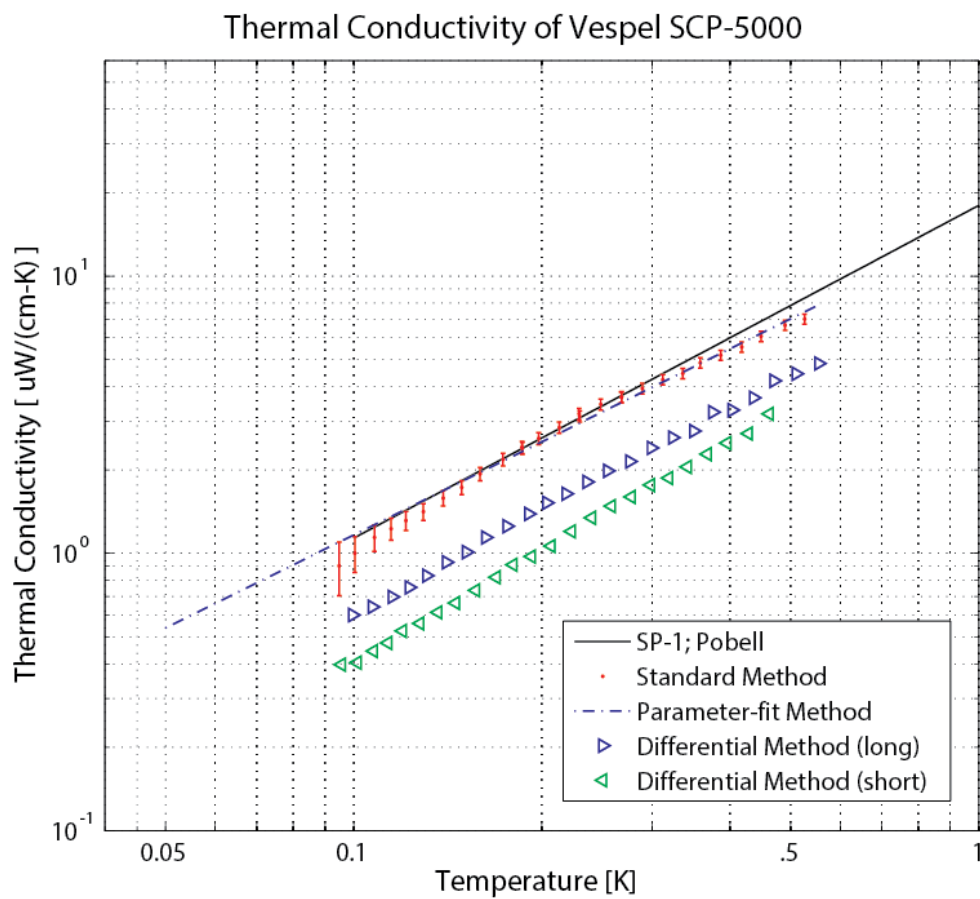


Figure 6: Thermal conductivity of Vespel SCP-5000 from 0.09K to 0.55K. This is compared to measurements of Vespel SP-1 taken from Pobell [2]. The agreement is very good.

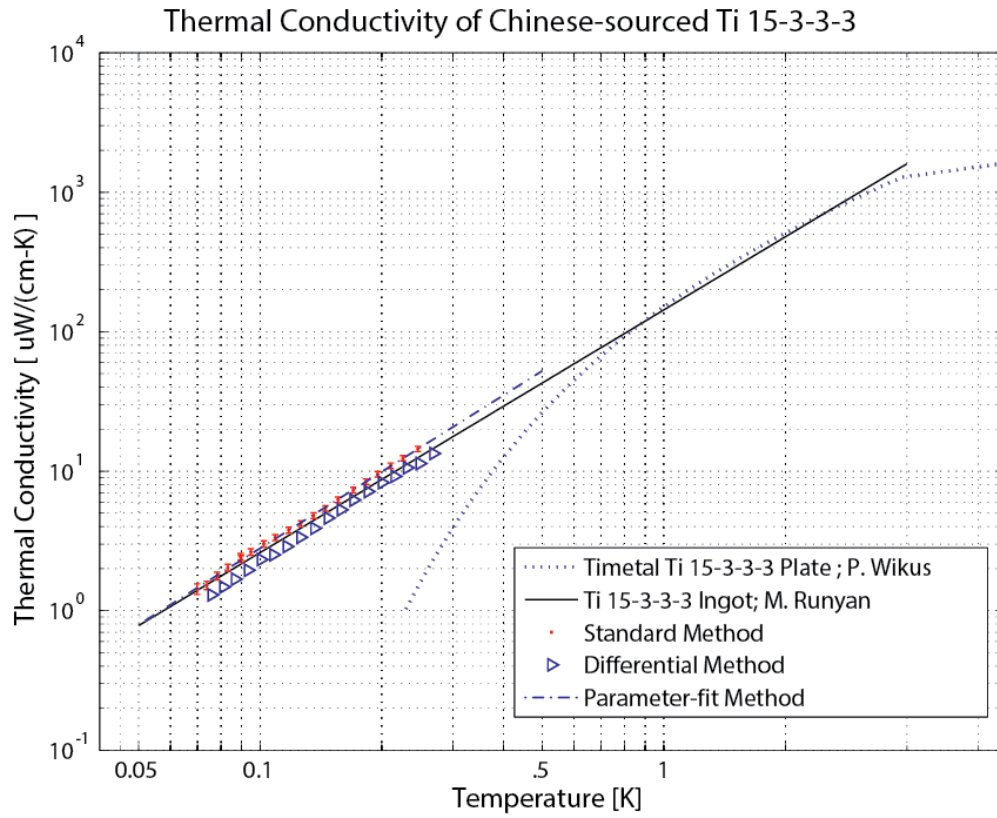


Figure 7: Thermal conductivity of ReTi Ti 15-3-3-3 from 0.07K to 0.3K. There is a slight discrepancy between the differential method and the parameter-fit/standard methods. The agreement with the Chinese-sourced Ti 15-3-3-3 sample measured by M. Runyan is good. The interesting thermal conductivity behavior exhibited by TIMETAL's Ti 15-3-3-3 plate measured by Wikus in [4] is not present in this sample.

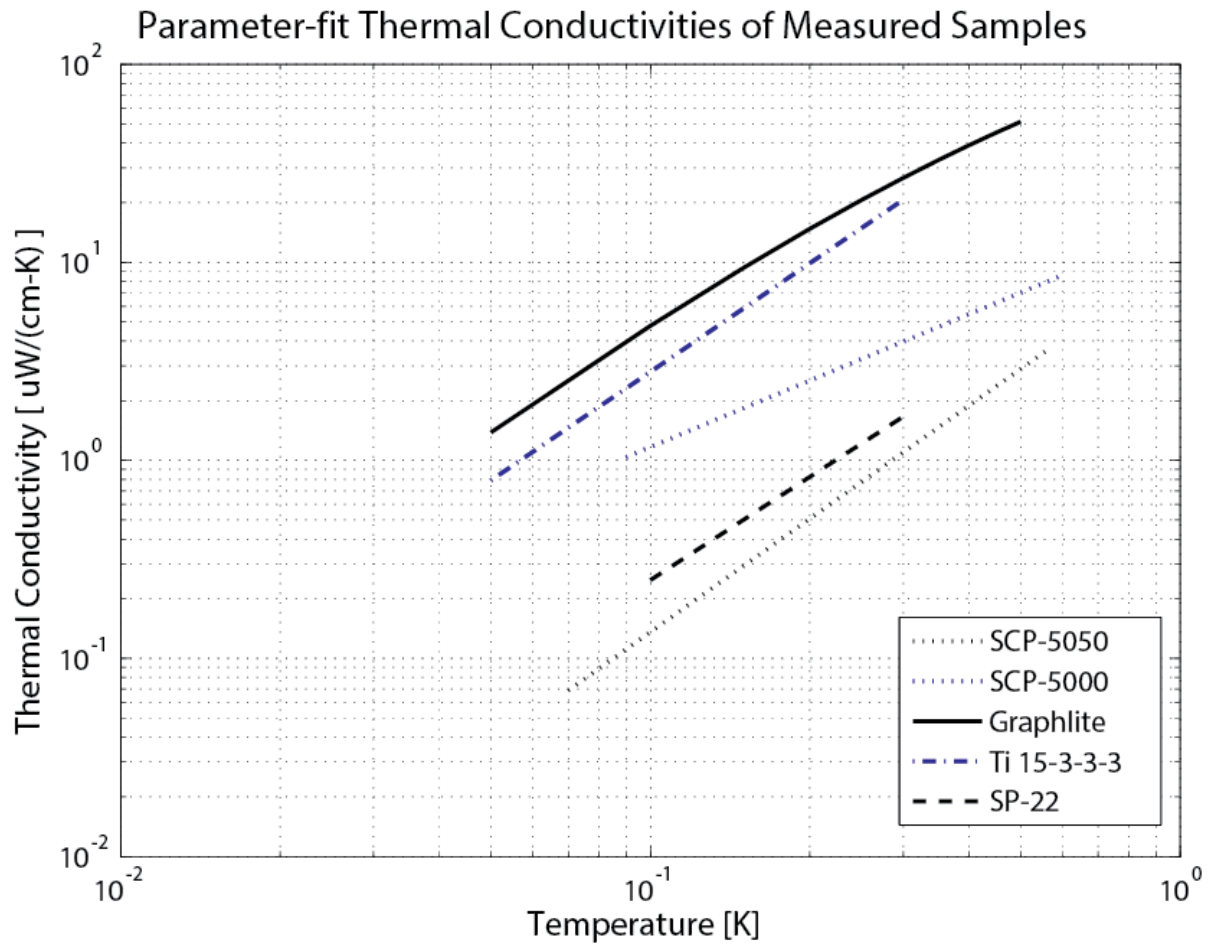


Figure 8: Compiled thermal conductivities of all measured materials.

References

- [1] J.R. Olson. Thermal Conductivity of Some Common Cryostat Materials between 0.05 and 2 K. *Cryogenics*, 33, 1993.
- [2] F. Pobell. *Matter and Methods at Low Temperatures*. Springer-Verlag, Heidelberg, Germany, second edition, 1992.
- [3] M.C. Runyan and W.C. Jones. Thermal Conductivity of Thermally-Isolating Polymeric and Composite Structural Support Materials between. *Cryogenics*, 48:448–454, 2008.
- [4] P. Wikus, S.A. Hertel, S.W. Leman, K.A. McCarthy, S.M. Ojeda, and E. Figueroa-Feliciano. The Electrical Resistivity and Thermal Conductivity of Ti 15V-3Cr-3Sn-3Al at Cryogenic Temperatures. *Cryogenics*, 2010.